

# Modeling and simulation of efficiency of cassava attrition peeling machine

J.C. Edeh<sup>1\*</sup>, O.S. Onwuka<sup>1</sup>, J.E. Chukwu<sup>2</sup>, B.N. Nwankwojike<sup>1</sup>

(1. Department of Mechanical Engineering, Michael Okpara University of Agriculture, Umudike, Abia State, Nigeria;

2. Department of Mechanical Engineering, Federal College of Education Technical, Umunze, Anambra State, Nigeria)

**Abstract:** A mechanistic based model for computing efficiency of an improved cassava attrition peeling machine was developed and evaluated in this study to enable performance predictions prior to fabrication. The model accounted for all relevant parameters affecting peeling with peeling efficiency established as a function of tuber mass, moisture content, drum speed, sphericity, peel thickness, number and surface area of peeling balls among others. The simulation model was developed using algebraic substitution/computation based algorithm. The comparative analysis validated the simulation model with the improved model's prediction error ranging from -0.006% to 0.011% resulting in over 99% prediction accuracy. Also, the simulation presented a user friendly interface that eliminated the computational rigors associated with error prone manual computations as a relief to researchers in the cassava processing sector. Hence, the improved peeling efficiency model and its simulation are recommended for developing varying capacities of cassava peelers required by end users in order to eliminate cost intensive trial and error associated with the empirical approach.

**Keywords:** cassava peeling, attrition, peeling efficiency, mechanistic model, simulation

**Citation:** Edeh, J. C., O. S. Onwuka, J. E. Chukwu and B. N. Nwankwojike. 2022. Modeling and simulation of efficiency of cassava attrition peeling machine. *Agricultural Engineering International: CIGR Journal*, 24(2): 166-183.

## 1 Introduction

Several operations are involved in cassava processing, which included peeling, washing, grating, boiling, parboiling, drying, milling, pressing, sieving, extrusion and frying (Igbeka et al., 1992; Kolawole et al., 2010; Jimoh and Olukunle, 2012). Mechanization of these operations reduces the drudgery in post-harvest processing. Virtually other cassava processing operations have been successfully and commercially mechanized with exception of cassava peeling. Works of researchers as reviewed by Egbeocha et al. (2016) were unable to exhaustively address the challenges of

dimensional disparities across varieties which limits the efficient mechanical peeling process. Cassava peeling operation has witnessed various stages of mechanization, all geared towards ensuring greater throughput capacity of peeled cassava to meet the ever increasing demand for processed cassava products (Alli and Abolarin, 2019). Yet adequate but efficient mechanized cassava peeling still pose a serious problem to the cassava processing industries in Nigeria and calls for serious attention. Good background knowledge of some engineering properties of cassava tubers articulated in machine development will complement in improving capacities and efficiencies of existing peelers.

Researchers of post-harvest processing machines have designed and manufactured many cassava peeling machines yet inadequate to address the problems of irregularities in shapes and sizes of cassava tubers across varieties. To account for these, most of them resorted to

---

**Received date:** 2020-06-30 **Accepted date:** 2021-11-24

**\*Corresponding author:** J. C. Edeh, Department of Mechanical Engineering, Michael Okpara University of Agriculture, Umudike, Abia State, Nigeria.

Tel: +2348037722756. Email: [engredehjohn@gmail.com](mailto:engredehjohn@gmail.com).

the pre-operational treatment of trimming, sorting and grading prior to peeling operation. The drudgery and inefficiency introduced by these initial treatments as observed by Ajibola and Babarinde (2016) cannot be overemphasized. For instance, in an automated cassava peeling system developed by Olukunle and Akunili (2012), the irregularities of the shapes were trimmed out to match the peeling unit of the machine and the operation resulted in high flesh loss (Olukunle and Jimoh, 2012). Adetan et al.(2006) developed a knife peeling machine that though spring loaded also removes the useful flesh in the peeling process as the knife shapes the irregular shaped cassava to suit the peeling unit of the machine. Olukunle et al.(2010), Alli and Abolarin (2019) emphasized that the peeling machine's output was dependent, among other things, on the variety, stage of maturity (age) and moisture content of the tubers.

However, an improved cassava attrition peeling machine devoid of pre-operational treatment and suitable for peeling irrespective of cassava tuber geometric properties, age, source and variety was developed evaluated and optimized (Edeh et al., 2020). It is desired to operate this machine with maximum efficiency and throughput, at minimum flesh loss and specific energy consumption possible. In addition, there is need for universal application of this concept in developing different capacities of peeling machine as may be desired by end users in the sector. Finally, to account for other relevant parameters not accounted for and to ensure universal applications, a physical law based model became imperative hence mechanistic evaluation of the attrition peeling principle became of the essence. Prediction of optimal operational parameters of this machine will make its use economical in terms of labour, time and energy requirement, thereby reducing the cost of cassava processing. These therefore, call for developing a realistic cassava peeling efficiency model for general application in the cassava processing industry.

Development of simulation for computation, prediction and optimization of systems is a growing trend in engineering since its implementations eliminates the huge economic investment of trial and error

approach in developing suitable systems and computational rigors of manual process. Calculation of Phase Diagrams software (CALPHAD) was developed and implemented by Sundman et al. (2015) in calculating properties of multi-component systems using databases of thermodynamic descriptions with models that are assessed from experimental data; Malozemov (2015) developed a software for the calculation and optimization of diesel operating processes and fuel supply while Lee and Park (2013) developed an optimization software system for nonlinear dynamics using the equivalent static loads method. Nwankwojike et al.(2016) developed mechanistic models for predicting specific energy consumption and throughput of palm nut–pulp separator. Each model's prediction accuracy was over 99 % with maximum prediction errors of 0,076 % and 0.03 % respectively. This high level of prediction accuracy affirmed the suitability of mechanistic models in systems characteristics predictions. Thus, among the objectives of this study is to develop models based on mechanistic approach for predicting cassava tuber peeling efficiency with the established significant cassava properties affecting peeling.

## 2 Materials and methods

A developed and fabricated improved cassava attrition peeling machine located in Michael Okpara University of Agriculture, Umudike, Abia State, Nigeria (5.4836 °N, 7.5483 °E) was used in this study (between August and October, 2019). C<sup>#</sup>(C-Sharp) and MATLAB version R2007b software were used in the simulation and implementation of the model. Cassava tubers accessed from farm of National Root Crop Research Institute, Umudike, Abia State, Nigeria (5.5 ° N, 7.5 ° E) were used for experimental validation.

### 2.1 Machine description.

The major components of the cassava attrition peeling machine are the frame, peeling unit, electric motor, water trough (bath) and peeled cassava discharging chute (Figure 1). The frame is formed from 5mm thick angle iron and served as the main supporting structure for mounting of other components of the machine. The peeling drum chamber consists mainly of a

rolled perforated aluminum plate of 2482 mm×400 mm×10 mm formed into a cylindrical drum and centrally mounted on a mild steel shaft which is a 1100mm long by 45mm diameter with three 400mm long angular aluminum bars of 10mm thickness welded to the inner surface. The bars are equidistantly spaced acting as

breaker baffles to check centrifugal effect thereby extending sticking speed. The perforations (6mm hole) were made at regular intervals of 4 holecm<sup>2</sup> such that the embossments enhance the frictional characteristics of the inner drum surface.

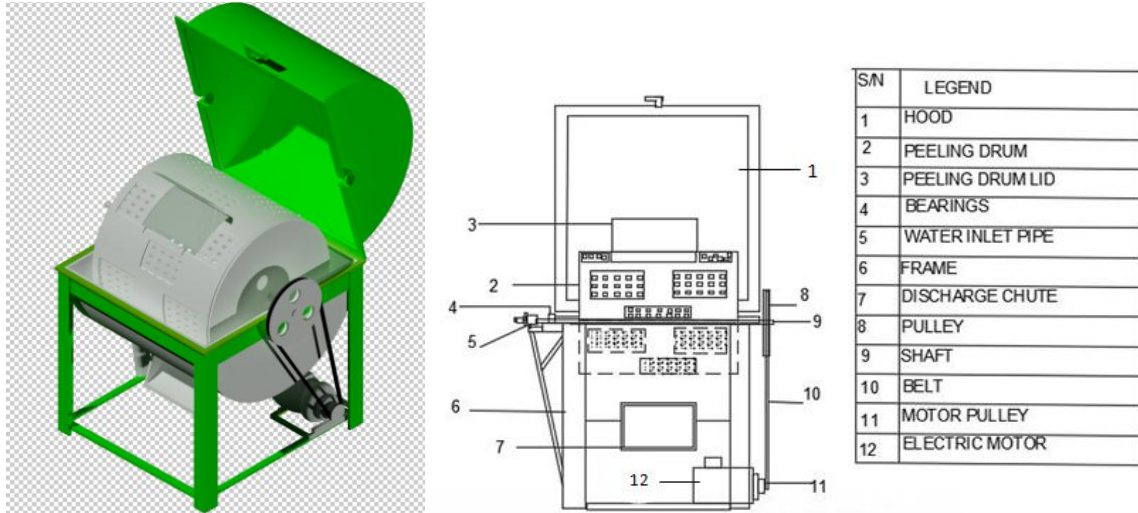


Figure 1 Modified Cassava Attrition Peeling Machine

The peeling drum closed at the ends was provide with a hinged feeding gate 400 × 300mm along with the length and discharge gate (slit) at one end. To provide mechanical strength against the twisting moment, the drum was reinforced on the outside with mild steel webbed plate and the whole assembly mounted with two outboard bearings on the structural frame. The peeling unit is partially submerged in a semi-cylindrical tank (serving as water bath and discharge unit) of diameter 500 mm and length 1050 mm welded to a structural stand, both made from 3mm and 5mm thick mild steel sheet and angular bar respectively. A geared electric motor of 3.73kW (8:1) mounted beneath the housing drives the peeling unit by means of pulley and belt arrangement. In the attrition peeler, peeling effects are enhanced by introduction of peeling balls of high frictional properties. The shape of the ball was investigated to be a critical factor for effective peeling. The peeling balls were produced from expanded mild steel sheet.

The egg-shaped peeling balls together with the embossed inner surface of the drum causes the uniform wearing of the cassava peel. Being a batch process operation, the cylindrical peeling drum impacts rotational motion on the balls freely mixed with the cassava and consequently create a tumbling effect in the drum that gives random relative motion hence effecting peeling. The egg shape of the balls makes it possible for depressions on the surface of the cassava to be engaged while the breaker baffles breaks the uniform angular speed which the loaded cassava attains at critical speed and this increases agitation, extending critical speed hence more peeling effect. Material removed from the surface of the cassava by abrasion, which has the form of flake and also tiny particles in pulpy matter, sinks through the perforation of the drum to the bottom of the housing trough serving as water bath and also prevents the clogging of nibbler balls. After satisfactory peeling for reduced peeling time, the peeled cassava together with the balls is evacuated through the slit at end of the drum into the evacuation chamber (where the balls are recovered and reintroduced for the next batch operation).

### 3 Model development

The mathematical model development process

In operation, a known mass of cassava for which other relevant properties are determined and estimated number of peeling balls are loaded through the gate into the peeling drum. The machine is energized through the prime mover causing a rotational motion of the drum.

involves a description of the basic mechanics of the machine by assigning symbols to its variables, derivation of the machine peeling efficiency from fundamental laws of geometry, mechanics, and verification of dimensional homogeneity of the developed model. Thereafter, a computer based simulation model was developed to eliminate the rigors of lengthy and error-prone manual computations. The developed simulation model was evaluated and validated at the Michael Okpara University of Agriculture, Umudike, Abia State of Nigeria (5.4836° N, 7.5483° E) by comparing different peeling efficiency of existing machines with model predicted peeling efficiency. The model was run with range of variables (some already established in the works of Nwankwojike et al. (2017) and the results were compared with the actual results obtained from the machines. Its mean square/ absolute errors, scatter index and correlation coefficient were determined to know how properly the model fits the measured data. The variables are factors affecting the modified cassava peeling machine and were classified as machine and crop factors. Machine factors included machine capacity (100 kg/batch), surface area (0.9361 m<sup>2</sup>), mass (50 g) and number of peeling balls (50-105), machine speed (25-80 r/min) among others while the crop factors comprised crop parameters like mass of cassava, surface area, moisture content, geometric mean diameter, sphericity, peel weight, tuber mechanical strength among others. Crop parameters were determined through direct measurement and application of already established relevant equations in the works of Nwachukwu and Simonyan (2015) and Nwankwojike et al. (2017) (Appendix A). The development of the model was based on some simplifying assumptions made in order to reduce the number of parameters involved to manageable level thereby reducing the complexity of the model.

The assumptions include;

1) Cassava tubers are irregular in shape and predominantly conical along the length with the mass of the tuber ranges between 0.3kg to 2kg.

2) True density of cassava is uniform and the same for both peel and flesh for any variety

3) The peeling balls are egg shaped ( $a = 0.002; b = 0.0022; c = 0.0032$ ) and of same material as the drum contributing 20 % of the peeling

4) Frictional force between the rotating drum and adjacent cassava tubers and peeling balls causes wear of tuber surface which gives rise to peeling. Hence peeling is by abrasion leading to wear.

5) Mass of the drum is negligible compared to the mass of cassava per batch.

Peeling efficiency is the ratio of throughput capacity to the theoretical capacity expressed as a percentage. Agrawal et al. (1987) gave the peeling efficiency,  $\eta_p$  (%) as

$$\eta_p = \frac{M_{pc}}{M_{pr} + M_{pc}} \times \frac{100}{1} \quad (1)$$

Where  $M_{pc}$  and  $M_{pr}$  are the mass of peel (kg) removed by the machine and mass of peel removed by hand after machine peeling (kg) respectively.

Peeling mass proportion according to Balami et al. (2012) is given as

$$p_w = \frac{M_{pc}}{M_s} \quad (2)$$

Where  $M_s$  is the total mass of peel, kg

Therefore

$$M_{pc} = p_w M_s \quad (3)$$

Hence, Equation 1 can be expressed as

$$\eta_p = \frac{p_w M_s}{M_r + p_w M_s} \times 100 \quad (4)$$

Attrition peeling is by wear of cassava tuber surface; according to Archard (1953) as reviewed by Zmitrowicz (2006), wear on frictional surfaces,  $u$  is directly proportional to applied normal load,  $W$  (N) and inversely proportional to the strength (hardness) of softest material in contact,  $H$  (Nmm<sup>-2</sup>), can be seen by the following relation

$$u = kW / H \quad (5)$$

Where  $k$  is non-dimensional expressed as wear coefficient (wear factor). This wear factor is expressed into a dimensional wear coefficient which is more widely used in Engineering as

$$u = k / H \quad (6)$$

Where  $u$  is the volumetric wear (mm<sup>3</sup>) resulting from the shift in unit distance (m) under unit load (N).

According to Engin (2013) if a solid material or a solid particle removes pieces by scratching or rubbing, this is defined as abrasion/attrition and is given as

$$u = \frac{2 \tan \theta}{\pi} \times \frac{W}{H} \quad (7)$$

Where:  $u$  is the wear volume( $\text{mm}^3$ ) and  $\theta$  is the cone angle ( $^\circ$ ).

If wear volume,  $u$  is replaced with  $Q$ , then Equation 7 becomes

$$Q = \frac{2 \tan \theta}{\pi} \times \frac{W}{H} \quad (8)$$

Sin et al.,(1979) gave a more simplified way of writing Equation 8 as

$$Q = \frac{kWL}{H} \quad (9)$$

Where  $L$  is the sliding distance (mm),  $H$  is the hardness of the softest contact surface ( $\text{Nmm}^{-2}$ ) and  $k$  was interpreted as the probability of forming wear debris from asperity encounter.

If the normal load ( $W$ ) replaced with a more convenient symbol ( $P_c$ ), Equation 9 changes to

$$Q = \frac{kP_cL}{H} \quad (10)$$

Where  $P_c$  represents the normal force on the cassava tubers and peeling balls, resulting from the torque of the rotating drum and causing them to slide along the drum of the machine.

Figure 2 shows the mechanics and forces (N) acting on the cassava and peeling balls as they rotate with the drum. Consider  $A$  as mass rotating in the drum of radius,  $R_d$  through inclined plane  $\theta$ .

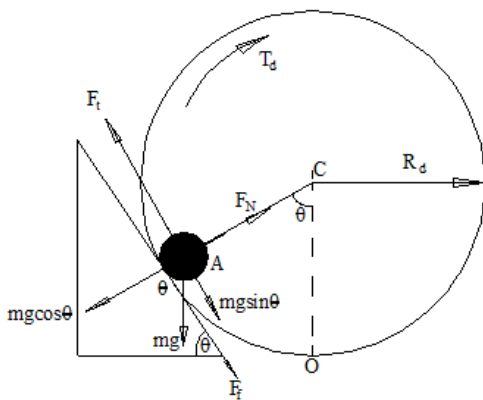


Figure 2 Modeled peeling drum of the cassava peeling machine

Let:

$F_t$  = Tangential force, N

$F_f$  = Frictional force, N

$F_N$  = Normal force, N

$mg$  = weight of the particle, N

$T_d$  = Torque on the drum, Nm

$R_d$  = Radius of the drum, m

Treating the drum as a rotating disk and the mass (mass of cassava and peeling ball) climbing an inclined plane (internal surfaces of the drum), basic mechanics relates tangential force with the drum torque and radius as thus

$$F_t = \frac{T_d}{R_d} \quad (11)$$

As the drum rotates carrying a mass  $m$ , the force diagram is approximated on an inclined plane at angle  $\theta$

Along the plane:

$$F_t = F_f + mg \sin \theta \quad (12)$$

Normal to the plane:

$$F_N = mg \cos \theta \quad (13)$$

When  $\theta = 0$  i.e. at the point  $O$  on the drum

$$F_t = F_f \text{ and } F_N = mg$$

It is this tangential component that keeps the cassava and peeling balls in place on the drum. As  $\theta$  increases to angle of repose, a throw force,  $F_{th}$  is developed as a result of gravity (and increasing angle,  $\theta$ ) beyond which the cassava and the peeling balls fall back (i.e. exceeding angle of repose). At this point the total throw force developed is given by

$$F_{th} = F_f + mg \sin \theta = F_f + (m_c + nm_b)g \sin \theta \quad (14)$$

Where  $F_{th}$  is the throw force,  $m_c$  is mass of cassava,  $m_b$  mass of peeling balls,  $n_b$  number of peeling balls. This throw force has been identified as major factor contributing to peeling.

At a limiting speed of the drum identified by Ezekwe (1979) as the sticking speed, the centrifugal effect overcomes the throw force and the cassava and peeling balls are kept (stuck) at the wall of the drum hence reducing peeling effect.

$$\omega^2 R_d = g \quad (15)$$

$$\omega = \sqrt{\frac{g}{R_d}} \text{ , in } \text{rads}^{-1} \quad (16)$$

Where  $\omega$  is the angular velocity of the drum.

Normal force and frictional force is related by

$$F_N = P_c = \frac{F_f}{\mu} \quad (17)$$

From Equation 12

$$F_f = F_t - mg \sin \theta = F_t - (m_c + nm_b)g \sin \theta \quad (18)$$

Substituting Equation 18 in 17

$$P_c = \frac{F_t - (m_c + nm_b)g \sin \theta}{\mu} \quad (19)$$

Power developed by the machine drum  $P_d$  is given as

$$P_d = \frac{2\pi N_d T_d}{60} \quad (20)$$

Where  $P_d$ ,  $N_d$  and  $T_d$  are the power, speed and torque of the rotating drum respectively.

But from Equation 11

$$T_d = F_t R_d \quad (21)$$

Combining Equations 20 and 21, we have

$$P_d = \frac{\pi N_d F_t R_d}{30} \quad (22)$$

Rearranging Equation 22, gives

$$F_t = \frac{30 P_d}{\pi N_d R_d} \quad (23)$$

This is the tangential force exerted on both the cassava tuber and the peeling balls by drum.

Substituting Equation 23 into 19 and subsequently into 10, gave

$$Q = \frac{k \left[ \left( \frac{30 P_d}{\pi N_d R_d} \right) - (m_c + nm_b)g \sin \theta \right] L}{\mu H} \quad (24)$$

Since the peeling balls are contributing 20% of the wear volume, therefore total volume of wear is

$$Q = \frac{1.2k \left[ \left( \frac{30 P_d}{\pi N_d R_d} \right) - (m_c + nm_b)g \sin \theta \right] L}{\mu H} \quad (25)$$

Dynamic strength (H) of cassava is the shear force,  $F_s (= F)$  per batch surface area of cassava tubers.

Since the machine is of batch process, there is need to approximate the surface area of cassava load per batch. The total surface area of cassava load per batch,  $S_{ac}$  is approximated assuming the drum is half loaded with the surface area of centre shaft neglected as half the surface area of the peeling drum minus surface area of peeling ball

$$S_{Tc} = S_{ad} - S_{ab} \quad (26)$$

Where  $S_{Tc}$ ,  $S_{ad}$  and  $S_{ab}$  are the total surface area of the cassava, surface area of the drum and surface area of the peeling balls respectively (in  $\text{mm}^2$ )

From basic geometric relations, surface area of the drum,  $S_{ad}$  is given by

$$S_{ad} = \pi R_d (R_d + L_d) \quad (27)$$

Therefore for half i.e.  $S_{ad}/2$

$$S_{ad} = \frac{1}{2} \pi R_d (R_d + L_d) \quad (28)$$

Where  $R_d$  and  $L_d$  are radius and length of the rotating drum respectively.

Surface area of egg shaped peeling balls can be approximated as

$$S_{ab} = 2\pi a^2 + \pi a \left[ \frac{b^2}{\sqrt{b^2 - a^2}} \cos^{-1} \left( \frac{a}{b} \right) + \frac{c^2}{\sqrt{c^2 - a^2}} \cos^{-1} \left( \frac{a}{c} \right) \right] \quad (29)$$

(<http://www.had2know.com>)

For n number of peeling balls  $n_b$  Equation 29 becomes

$$S_{ab} = 2\pi n_b a^2 + \pi n_b a \left[ \frac{b^2}{\sqrt{b^2 - a^2}} \cos^{-1} \left( \frac{a}{b} \right) + \frac{c^2}{\sqrt{c^2 - a^2}} \cos^{-1} \left( \frac{a}{c} \right) \right] \quad (30)$$

Where a, b, c are the equatorial, short polar and long polar radius respectively.

Combing Equations 27 and 29, total surface area of cassava load per batch,  $S_{Tc}$  is given by

$$S_{Tc} = \frac{1}{2} \pi R_d (R_d + L_d) - \left\{ 2\pi n_b a^2 + \pi n_b a \left[ \frac{b^2}{\sqrt{b^2 - a^2}} \cos^{-1} \left( \frac{a}{b} \right) + \frac{c^2}{\sqrt{c^2 - a^2}} \cos^{-1} \left( \frac{a}{c} \right) \right] \right\} \quad (31)$$

Dividing Equation 23 by Equation 31, dynamic strength of cassava is given as

$$H = \frac{30 P_d}{\pi N_d R_d \left[ \frac{1}{2} \pi R_d (R_d + L_d) - \left\{ 2\pi n_b a^2 + \pi n_b a \left[ \frac{b^2}{\sqrt{b^2 - a^2}} \cos^{-1} \left( \frac{a}{b} \right) + \frac{c^2}{\sqrt{c^2 - a^2}} \cos^{-1} \left( \frac{a}{c} \right) \right] \right\} \right]} \quad (32)$$

Equation 32 gives the dynamic strength (H) of the softest contact surface.

But volume of wear Q can also be written as

$$Q = \frac{M_s}{\rho_p} \quad (33)$$

Where  $M_s$  and  $\rho_p$  are mass and density of wear (peel) respectively

Substituting Equation 33 into Equation 25, gives

$$\frac{M_s}{\rho_p} = \frac{1.2k \left[ \left( \frac{30 P_d}{\pi N_d R_d} \right) - (m_c + nm_b)g \sin \theta \right] L}{\mu H} \quad (34)$$

$$M_s = \frac{1.2k \rho_p \left[ \left( \frac{30 P_d}{\pi N_d R_d} \right) - (m_c + nm_b)g \sin \theta \right] L}{\mu H} \quad (35)$$

Substituting for H in Equation 35 implies

$$M_s = \frac{1.2k \rho_p L \left[ \left( \frac{30 P_d}{\pi N_d R_d} \right) - (m_c + nm_b)g \sin \theta \right] \pi N_d R_d \left[ \frac{1}{2} \pi R_d (R_d + L_d) - \left\{ 2\pi n_b a^2 + \pi n_b a \left[ \frac{b^2}{\sqrt{b^2 - a^2}} \cos^{-1} \left( \frac{a}{b} \right) + \frac{c^2}{\sqrt{c^2 - a^2}} \cos^{-1} \left( \frac{a}{c} \right) \right] \right\} \right]}{\mu (30 P_d)} \quad (36)$$

Equation 36 is the mass (weight) in kg of cassava peel and flesh worn out

According to Archard (1953) and Vera-Cardenas et

al. (2017) wear factor  $k$  can be a property of the material set, sliding conditions, surface topography and environment among otherthings. Considering factors like the moisture content of the cassava at any time ( $\varphi_c$ ), peel thickness, sphericity and Geometric Mean Diameter ( $D_g$ ) as most important factors among others.

Koocheki et al. (2007) gave the relation between cassava sphericity,  $D_g$  and its major diameter as

$$\text{Sphericity} = \frac{D_g}{a_i} \tag{37}$$

Denoting sphericity with  $\phi$  for convenience  $\phi =$

$$\frac{D_g}{a_i} = \frac{(a_i b_i c_i)^{1/3}}{a_i} \tag{38}$$

Where  $D_g$  and  $a_i$  are the geometric mean diameter (MD) and major diameter of tuber respectively.

Brooker et al.(1974) summarized the relationship between equilibrium moisture content, relative humidity and temperature as

$$MR = \frac{\varphi_c - \varphi_e}{\varphi_i - \varphi_e} \tag{39}$$

Where  $MR$ ,  $\varphi_c$  and  $\varphi_i$  are the moisture ratio, equilibrium moisture content and initial moisture content of cassava after harvest.

Teter (1987) gave the following relation for  $MR$

$$MR = e^{-(xt^y)} \tag{40}$$

Where  $x = 0.026 - 0.0045h + 0.01215T$

$$y = 0.013362 + 0.194h - 0.00017h^2 + 0.009468T$$

$t =$  Drying time (seconds)

And  $T$  and  $h$  are air temperature ( $^{\circ}C$ ) and relative humidity (%).

Parra-Coronado et al., (2008) and Moreno et al.,(2014)gave the relationship for equilibrium moisture as

$$\varphi_e = 0.01Ae^{Bc} \tag{41}$$

$$\text{Where } A = 727.44h + 599.9h^2 + 475.64h^3$$

$$B = -0.0143 - 0.0771h + 0.132h^2 - 0.157h^3$$

$$- 0.0731h^4$$

$$c = (T + 81.64)$$

Substituting Equations40 and 41into Equation 39,

$$e^{-(xt^y)} = \frac{\varphi_c - 0.01Ae^{Bc}}{\varphi_i - 0.01Ae^{Bc}} \tag{42}$$

From Equation 42

$$\varphi_c = e^{-(xt^y)} [\varphi_i - 0.01Ae^{Bc}] + 0.01Ae^{Bc} \tag{43}$$

Although the dimensional analysis of the peel thickness and geometric mean diameter showed an inverse and direct relationship respectively with peeling efficiency, however peeling efficiency forms a dimensionless quantity with moisture content with direct relationship.

Incorporating these into Equation 4, the peeling efficiency becomes

$$\eta_p = \frac{\varphi_c D_g p_w M_s}{p_{th}(M_r + p_w M_s)} \tag{44}$$

Where  $P_{th}$ is the peel thickness (mm).

The sliding distance  $L$  is the total distance travelled by the cassava load per batch per a one complete peeling process. For one revolution of the drum, the cassava load travel a total distance equal to half of circumference of the drum.

Thus for the revolution of the drum

$$L = \frac{2\pi R_d}{2} = \pi R_d \tag{45}$$

Thus for  $n$  number of revolution of the drum  $n_d$

$$L = \pi n_d R_d \tag{46}$$

Combining Equations 36 and 45 and substituting same into Equation 44, gives

$$\eta_p = \frac{p_w \varphi_c D_g \left[ \frac{1.2k\rho_p \pi n_d R_d \left( \left( \frac{30P_d}{\pi N_d R_d} \right) - (m_c + nm_b) g \sin \theta \right) \pi N_s r_d \left[ \frac{1}{2} \pi R_d (R_d + L_d) - (2\pi n_b a^2 + \pi n_b a \left[ \frac{b^2}{\sqrt{b^2 - a^2}} \cos^{-1} \left( \frac{a}{b} \right) + \frac{c^2}{\sqrt{c^2 - a^2}} \cos^{-1} \left( \frac{a}{c} \right) \right] \right]}{\mu(30P_d)} \right]}{p_{th}(M_r + p_w \left[ \frac{1.2k\rho_p \pi n_d R_d \left( \left( \frac{30P_d}{\pi N_d R_d} \right) - (m_c + nm_b) g \sin \theta \right) \pi N_s r_d \left[ \frac{1}{2} \pi R_d (R_d + L_d) - (2\pi n_b a^2 + \pi n_b a \left[ \frac{b^2}{\sqrt{b^2 - a^2}} \cos^{-1} \left( \frac{a}{b} \right) + \frac{c^2}{\sqrt{c^2 - a^2}} \cos^{-1} \left( \frac{a}{c} \right) \right] \right]}{\mu(30P_d)} \right])} \tag{47}$$

$$\text{For } S_{Tc} = \frac{1}{2} \pi R_d (R_d + L_d) - \left\{ (2\pi n_b a^2 + \pi n_b a \left[ \frac{b^2}{\sqrt{b^2 - a^2}} \cos^{-1} \left( \frac{a}{b} \right) + \frac{c^2}{\sqrt{c^2 - a^2}} \cos^{-1} \left( \frac{a}{c} \right) \right] \right\}$$

substituting that in Equation (47)

$$\eta_p = \frac{p_w \varphi_c D_g \left[ 1.2\pi^2 k \rho_p n_d N_d R_d^2 \left( \left( \frac{30P_d}{\pi N_d R_d} \right) - (m_c + nm_b) g \sin \theta \right) S_{Tc} \right]}{p_{th} \left[ 30\mu P_d M_r + p_w \left( 1.2\pi^2 k \rho_p n_d N_d R_d^2 \left( \left( \frac{30P_d}{\pi N_d R_d} \right) - (m_c + nm_b) g \sin \theta \right) S_{Tc} \right) \right]} \tag{48}$$

The dimensional homogeneity of the peeling efficiency of Equation 48 is analyzed as shown

$$M^x L^y T^z = \frac{L \left[ ML^{-3} T^{-1} \cdot L^2 \left( \frac{ML^{-2} T^{-3}}{LT^{-1}} - MLT^{-2} \right) L^2 \right]}{L \left[ ML^{-2} T^{-3} \cdot M + ML^{-3} T^{-1} \cdot L^2 \left( \frac{ML^{-2} T^{-3}}{LT^{-1}} - MLT^{-2} \right) L^2 \right]}$$

$$M^x L^y T^z = \frac{L(ML^{-1} T^{-1} \cdot MLT^{-2} \cdot L^2)}{L(M^2 L^2 T^{-3} + MLT^{-1} \cdot MLT^{-2})}$$

$$M^x L^y T^z = \frac{M^2 L^3 T^{-3}}{L(M^2 L^2 T^{-3} + M^2 L^2 T^{-3})}$$

$$M^xL^yT^z = \frac{1 M^2L^3T^{-3}}{2 M^2L^3T^{-3}}$$

$$M^xL^yT^z = 1/2 M^0L^0T^0, \quad x=0, y=0, z=0$$

Hence the developed equation of peeling efficiency is dimensionally homogenous.

### 4 Results and discussion

It was observed from Equation 48, that peeling efficiency is a function of crop, machine and operational parameters, thus:

$$\text{Peeling efficiency, } \eta_p = f(N_d, R_d, M_c, M_r, m_b, n_b, p_w, \rho_p, \theta, \mu, k, \varphi_c, D_g, L_d, S_{TC}, P_d, P_{th}, g)$$

The input parameters (predictors) were varied for five different capacities of the cassava attrition peeling

machine and peeling efficiency computed based on Equation 48. Some of the variables were extracted from the works of Nwankwojike et al.(2017) (Appendix A). Table 1 shows the prediction of peeling efficiency model.

Though the peeling efficiency was computed using manual approach (Table 1) but there were a lot of computational rigours due to the model complexity and this approach was error prone. Moreover, individual effect of variables on peeling efficiency could not be easily determined. Therefore, simulation model with user friendly computer interface for implementing the model was developed.

**Table 1 Prediction of PE(η<sub>p</sub>) using the developed models**

Predictor	Capacities evaluated				
	I	II	III	IV	V
N <sub>d</sub> (r/min)	45	49	48	45	45
R <sub>d</sub> (m)	0.38	0.38	0.38	0.38	0.38
L <sub>d</sub> (m)	0.60	0.60	0.60	0.60	0.60
M <sub>c</sub> (kg)	100	85	80	85	70
M <sub>r</sub> (kg)	0.05	0.05	0.05	0.05	0.05
P <sub>w</sub>	0.92	0.94	0.92	0.93	0.92
ρ <sub>p</sub> (kg/m <sup>3</sup> )	1.12	1.12	1.13	1.20	1.11
P <sub>d</sub> (W)	2328.78	2328.30	2028.45	2328.67	2028.19
n <sub>b</sub>	104	100	96	12	100
m <sub>b</sub> (kg)	0.050	0.050	0.050	0.050	0.050
Θ (deg)	70	75	68	75	75
μ	0.3	0.3	0.28	0.28	0.30
K	10 <sup>-4</sup>	10 <sup>-4</sup>	10 <sup>-4</sup>	10 <sup>-4</sup>	10 <sup>-4</sup>
S <sub>TC</sub> (m <sup>2</sup> )	0.9361	0.9361	0.9361	0.9361	0.9361
D <sub>g</sub>	0.0442	0.0458	0.0463	0.0526	0.0466
P <sub>th</sub> (m)	0.0019	0.0024	0.0024	0.0023	0.0029
φ <sub>c</sub> (%)	72.69	84.00	73.83	63.50	63.33
g (ms <sup>-2</sup> )	9.81	9.81	9.81	9.81	9.81
η <sub>p</sub> (%)	95.02	92.98	95.27	94.73	91.12

#### 3.1 Simulation model

The simulation-model interface to implement the computation of peeling efficiency (%) level of the process and enables the user to ascertain specific effect of each parameter on the efficiency of any cassava attrition peeling machine under investigation was

developed.

In the simulation building, the peeling efficiency Equation 48 was broken down to sixteen sub equations (Appendix B) and assembled into three entities.

Entities: (BODMAS)

$$1,2k\rho_p\pi n_d R_d \left[ \left( \frac{30P_d}{\pi N_d R_d} \right) - (m_c + nm_b)g \sin\theta \right] \pi N_s r_d \left| \frac{1}{2} \pi R_d (R_d + L_d) \right. \\ \left. \left\{ \left( 2\pi n_b a^2 + \pi n_b a \left[ \frac{b^2}{\sqrt{b^2 - a^2}} \cos^{-1} \left( \frac{a}{b} \right) + \frac{c^2}{\sqrt{c^2 - a^2}} \cos^{-1} \left( \frac{a}{c} \right) \right] \right\} \mu (30P_d) \right.$$

The control interface using the entities as the basic parameters for development (Figures 3-5) with

combination of the user input parameters allows the users to navigate through the software simulation model.

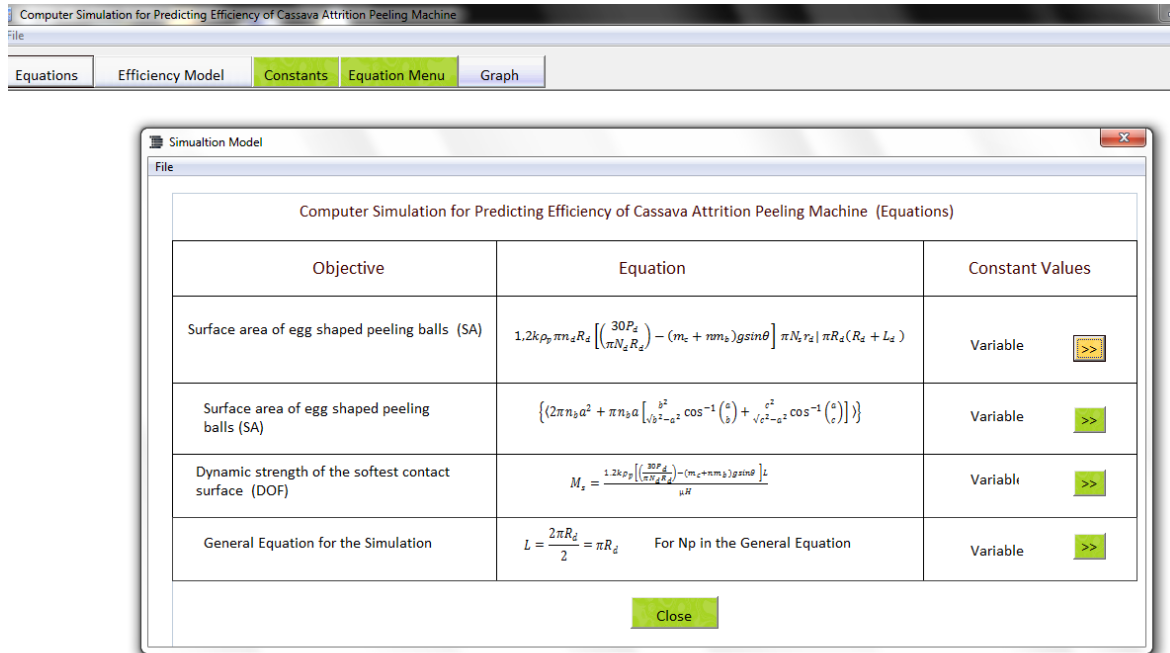


Figure 3 Model entities (BODMAS) composite interface

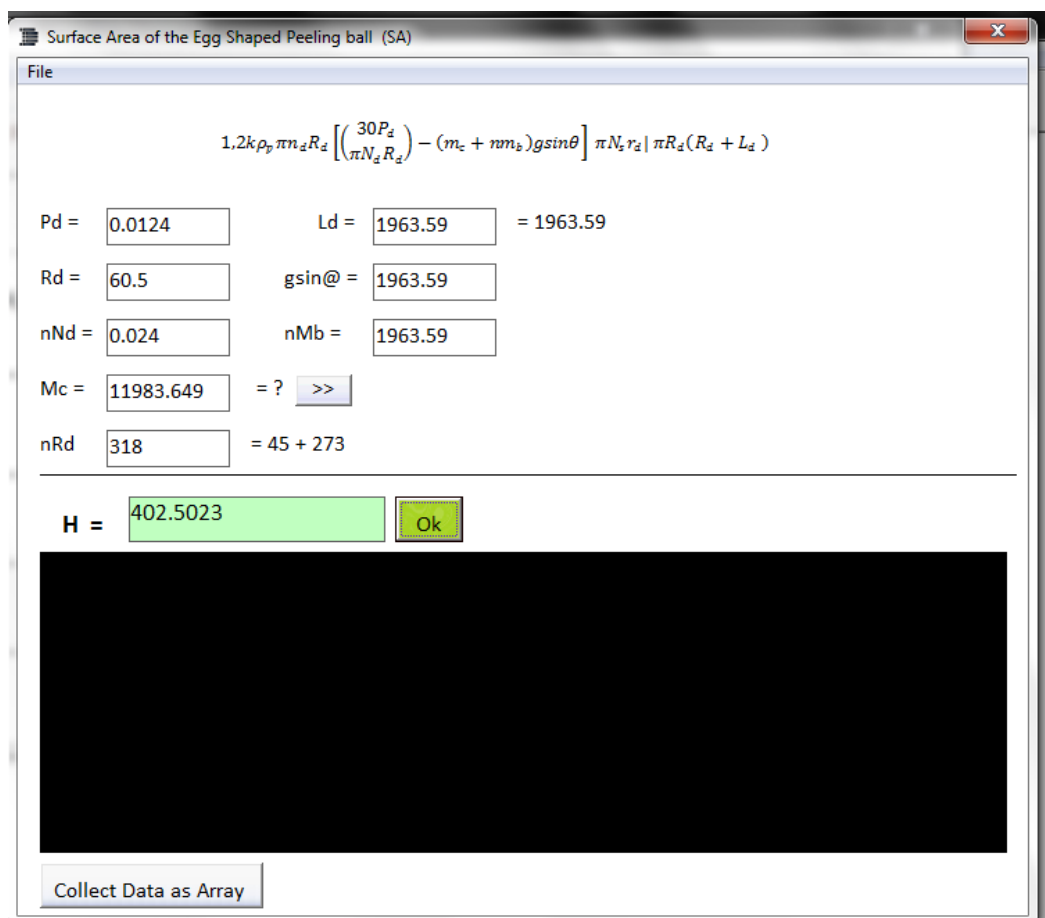


Figure 4 Model entities I component interface

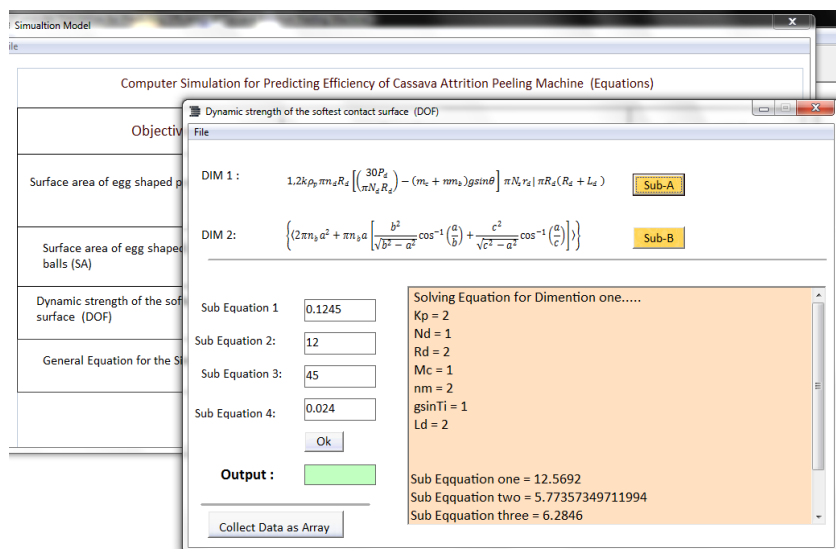


Figure 5 Dynamic strength component interface

Figure 6 shows the peeling efficiency simulation interface which upon input of the variables as prompted runs the underlying sub-programs(entities) and display the efficiency for the set of given input parameters.

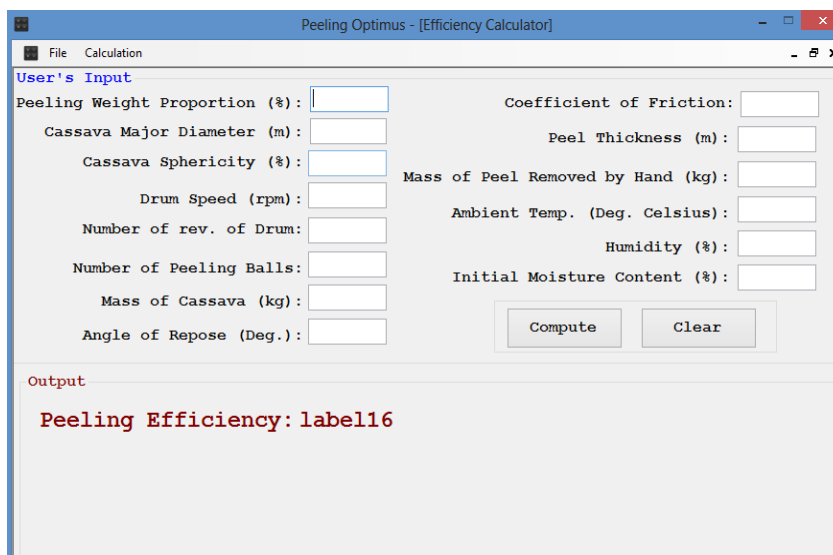


Figure 6 Peeling efficiency simulation interface

Figure 7 shows the specific effect of varying the input parameters in the simulation

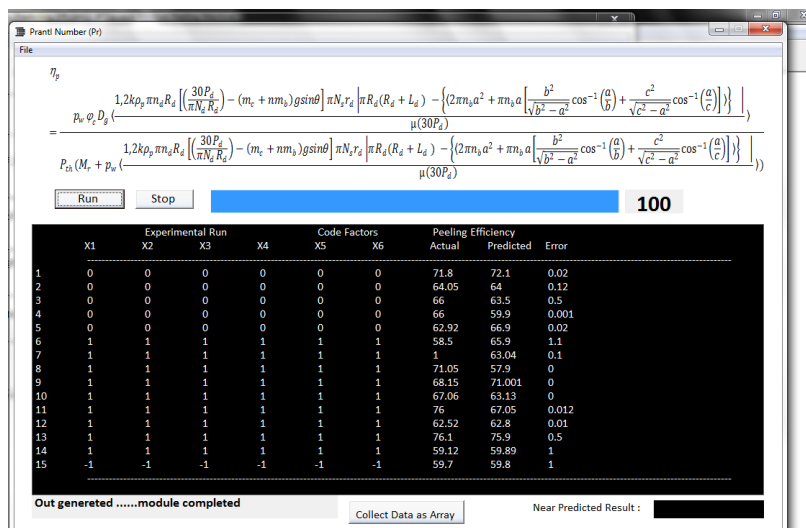


Figure 7 Specific effect of input parameters variation on the simulation

### 3.2 Model validation

Experimental test carried out on five trials (capacities I-V) of the developed machine was juxtaposed with the result of the simulation (using the values of variables of Table 1) as shown in Table 2. The peeling efficiency of the machine was determined from Equations 4. Table 2 therefore, showed the comparison between the actual experiment and models prediction.

**Table 2 Comparison of experimental values and model prediction of peeling efficiency**

Test	Peeling Efficiency (%)		
	Actual	Predicted	Error (%)
I	94.45	95.02	-0.006
II	93.00	92.98	0.000
III	96.23	95.27	0.010
IV	95.01	94.73	0.003
V	90.70	91.12	-0.004

Analysis of variance of this model revealed over 99% prediction accuracy (prediction error range of -0.006% to 0.011%). Its mean square/ absolute errors, scatter index and correlation coefficient were determined as 0.013/0.006, 0.170 and 97.16% respectively.

Also the simulation model showed slight improvement on the peeling efficiency potentials and stability of this machine over the response surface simulation records of 88.4% by Edeh et al. (2018). This is obvious since the simulation was developed base on mechanistic models which accounted for all operational and performance parameters of the machine unlike its data based response surface simulation that considered six operational factors. Therefore, the use of manual computation with attendant complexities should be discouraged.

### 4 Conclusion

Mechanistic model for predicting the peeling efficiency of a cassava attrition peeling machine of any given capacity prior to fabrication was developed and comparatively evaluated using experimental/field data of an existing improved cassava attrition peeling machine. Test for homogeneity revealed that the developed mechanistic model which accounted for all relevant parameters affecting peeling is dimensionally homogeneous hence suitable for application to ensure

effective design analysis of machinevarying component parameters. The simulation model was developed using algebraic substitution/computation based C-sharp program. Analysis of this model revealed that its predictions reckon with the actual performance of the test specimens up to 99% confidence interval. Thus, the implementable simulation prediction model presented a user friendly interface that eliminated the computational rigors associated with error prone manual computations as a relief to researchers in cassava processing sector and should be used in the replication of different sizes of cassava attrition peeler in order to ensure optimal operation after fabrication.

### Acknowledgements

Technical supports and programming assistances of Engr. Edeh C.C and Olise P. are highly acknowledged. We also wish to state that there is no conflict of interest of any kind regarding this work.

### References

- Adetan, D. A, L. O.Adekoya and O. L. Aluko. 2006. Theory of a mechanical method of peeling cassava tubers with knives. *International Agrophysics*20: 269-276.
- Agrawal, Y. C. A. Hiran and A. S. Galundia1987. Ginger peeling machine parameters. *Agricultural Mechanization in Asia, Africa and Latin America*18(2): 59-62.
- Ajibola, W.A. and F. Babarinde.2016.Design and fabrication of a cassava peeling machine. *International Journal of Engineering Trends and Technology*, 42(2): 60-64
- Alli, O.D., and M. S. Abolarin. 2019. Design modification of a cassava attrition peeling machine. *Journal of Physics: Conference Series*,1378: 032029
- Archard, J.F.1953.Contact and rubbing of flat surfaces.*Journal of Applied Physics*24(8): 981-988.
- Balami, A. A., I. A.Mohammed, S. E.Adebayo, D. Adgidzi, and A. A. Adelemi. 2012. The relevance of some engineering properties of cocoyam (*Colocasiaesculenta*) in the design of post- harvest processing machinery. *Academic Research International*, 2(3): 53- 59.
- Brooker, D B.,F. W.Bakker-Arkema and C. W.Hall. 1974. Drying cereal grains. Westport: Avi Publishing Co. Inc.
- Edeh, J. C.,B. N. Nwankwojike and F.I. Abam. 2018.Parametric optimization of improvedcassava attrition peeling machine

- using RSM based desirability function. *International Review of Mechanical Engineering*, 12 (10): 823-836.
- Edeh, J.C., B.N. Nwankwojike and F.I. Abam. 2020, Design Modification and Comparative Analysis of Cassava Attrition Peeling Machine. *Agricultural Mechanization in Asia, Africa and Latin America (AMA)* 51 (1): 63-71
- Egbeocha, C.C., S.N. Asoegwu, and N.A.A. Okereke. 2016. A Review on Performance of Cassava Peeling Machines in Nigeria. *Futo Journal Series (FUTOJNLS)* 2(1): 140 – 168.
- Engin, I. C. 2013. Theories on rock cutting, grinding and polishing mechanisms. In *Tribology in Engineering*. Ed. H. Pihtili, ch. 10, 185-208. Rijeka, Croatia: In Tech
- Ezekwe, G.O. 1979. Mechanising cassava peeling: The PRODA Cassava Nibbling Machine, PRODA Technical Reports, No. 1:1 -20. <http://www.had2know.com>. Surface area of an egg. Accessed February 5, 2017.
- Igbeka, J.C., M. Jory, and D. Griffon. 1992. Selective mechanization for cassava processing. *Journal of Agricultural Mechanization in Asia, Africa and Latin America (AMA)*, 23 (1): 45-50.
- Jimoh, M. O. And O.J. Olukunle. 2012. An automated cassava peeling system for the enhancement of food security in Nigeria. *Nigerian Food Journal* 30(2): 73-79.
- Kolawole, P. O., L. Agbetoye, and S. A. Ogunlowo. 2010. Sustaining world food security with improved cassava processing technologies: The Nigerian experience. *Sustainability*, 2(12) 3681- 3694.
- Koocheki, A. S., M.A. Razavi, E. Milani, T. M. Moghadam, M. Abedini, S. Alamatyian, and S. Izadkhan. 2007. Physical properties of water melon seed as a function of moisture content and variety. *International Agro Physics* 21: 349-359.
- Lee, H. A., and G. J. Park. 2013. Development of an optimization software system for nonlinear dynamics using the Equivalent Static Loads Method. *10th World Congress on Structural and Multidisciplinary Optimization*, 1-10. Orlando, Florida, USA, 19-24.
- Malozemov, A.A. 2015. Development of software for calculation and optimization of diesel operating processes and fuel supply. *Procedia Engineering*, 129: 724-730.
- Moreno, F.L., A. Parra-Coronado and J.H. Camacho-Tamayo. 2014. Mathematical simulation parameters for drying of cassava starch pellets. *Engenharia Agrícola*, 34(6): 1234-1244.
- Nwachukwu, I. D, and K.J. Simonyan. 2015. Some engineering properties of cassava tuber related to its peeling mechanization. *Umudike Journal of Engineering and Technology (UJET)*, 1(1): 12-24.
- Nwankwojike, N.B., O. S. Onwuka, J. C. Agwunwamba, and C. J. Adama. 2016. Mechanistic models for predicting specific energy consumption and throughput of palm nut-pulp separator. *Applied Mathematical Modelling*, 40(11-12): 5978-5987.
- Nwankwojike, B. N., F. I. Abam and J. C. Edeh. 2017. Modeling and parametric analysis of peel mass of cassava tubers. In *Proc. of 18<sup>th</sup> International Conference of NIAE on Dynamics of Agricultural Engineering for Food and Agro-Industrial Raw Materials Production for Economic Recovery in Nigeria*, 38: 225-230. Umudike, October
- Olukunle, O. J., A.S. Ogunlowo, and L. Sanni. 2010. The search for effective cassava peeler. *The West Indian Journal* 32 (1 & 2): 42-47.
- Olukunle, O. J. and M. O. Jimoh. 2012. Comparative analysis and performance evaluation of three cassava peeling machines. *International Research Journal of Engineering Science, Technology and Innovation*, 1(4): 94 -102.
- Olukunle, O.J. and B.O. Akinnuli. 2012. Performance evaluation of a single action cassava peeling machine. *Journal of Emerging Trends in Engineering and Applied Sciences* 3(5): 806–811.
- Parra-Coronado, A., G. Roa-Mejía, and C.E. Oliveros-Tascón. 2008. SECAFEPart I: Modeling and mathematical simulation in the mechanical drying of parchment coffee. *Revista Brasileira de Engenharia Agrícola*. 12(4): 415-427.
- Sin, H., N. Saka, and N.P. Suh. 1979. Abrasive wear mechanisms and the grit size effect. *Wear*, 55(1): 163-190.
- Sundman, B., U. R. Kattner, M. Palumbo, and S. G. Fries. 2015. Open Calphad - A free thermodynamic software. *Integrating Materials and Manufacturing Innovation* 4(1): 1-15.
- Teter, N. 1987. Paddy drying manual. Agricultural Services Bulletin No. 70. Rome, Italy. FAO.
- Vera-Cardenas, E. E., R. Lewis, and T. Slatter. 2017. Sliding wear study on the valve-seat insert contact. *Open Journal of Applied Sciences*, 7(2): 42-49.
- Zmitrowicz, A. 2006. Wear patterns and laws of wear – A review. *Journal of Theoretical and Applied Mechanics*, 44(2) 219-253.

**Appendix A1: UMUCAS-36 Variety**

Sample	L (mm)	M <sub>c</sub> (g)	V <sub>c</sub> (cm <sup>3</sup> )	ρ <sub>s</sub> (g/cm <sup>3</sup> )	R <sub>th</sub> (mm)			GMD (mm)	Sphericity φ	S <sub>a</sub> (mm <sup>2</sup> )	P <sub>th</sub> (mm)	V <sub>p</sub> (mm <sup>3</sup> )	M <sub>Pt</sub> (g)	M <sub>Pa</sub> (g)
					a	b	C							
1	385	610	565	1.08	63	60	29	47.86	0.76	7198.98	1.71	12310.25	104.37	99.44
2	437	920	1035	0.89	83	72	46	65.02	0.78	13287.91	1.84	24449.75	136.38	125.19
3	358	675	624	1.08	80	63	37	57.13	0.71	10258.86	3.16	32452.2	196.59	186.05
4	315	365	349	1.05	58	50	33	45.74	0.79	6575.86	3.07	20165.96	135.22	121.78
5	366	565	472	1.2	73	62	32	52.52	0.72	8668.04	2.95	25570.71	197.24	182.23
6	340	345	305	1.13	66	42	32	44.6	0.68	6251.34	1.54	9627.07	67.92	64.72
7	311	510	498	1.02	60	61	22	43.18	0.72	5860.66	3.39	19848.12	147.61	117.73
8	259	365	349	1.05	55	52	39	48.14	0.88	7282.8	1.83	13327.52	72.95	73.87
9	315	245	214	1.14	47	36	31	37.43	0.8	4404.05	1.43	6297.79	53.57	49.21
10	398	315	285	1.11	51	44	22	36.68	0.72	4229.69	2.13	8995.13	100.46	87.69
11	226	382	352	1.09	74	60	22	46.05	0.62	6666.25	1.45	9666.06	46.61	45.6
12	294	300	258	1.16	52	47	32	42.76	0.82	5747.93	1.35	7740.55	58.9	47.7
13	218	485	453	1.07	74	67	30	52.98	0.72	8823.27	3.05	26910.97	112.93	112.7
14	328	250	186	1.34	57	40	43	46.11	0.81	6682.62	1.33	8910.16	72.48	63.47
15	296	285	213	1.34	54	47	22	38.22	0.71	4591.49	1.47	6734.19	65.26	57.76
16	224	375	314	1.19	66	54	23	43.44	0.66	5930.91	1.33	7907.88	44.27	42.05
17	211	295	281	1.05	61	48	28	43.44	0.71	5931.49	1.4	8304.09	37.83	36.2
18	198	195	140	1.39	51	40	28	38.51	0.76	4661.62	1.46	6805.96	43.48	41.24
19	227	225	235	0.96	54	45	35	43.98	0.81	6078.47	1.43	8692.21	39.38	44.11
20	218	195	166	1.17	53	44	25	38.78	0.73	4725.6	1.28	6064.52	36.65	37.76
21	195	225	196	1.15	55	45	23	38.47	0.7	4651	1.26	5844.76	30.92	30.56
22	205	165	152	1.09	49	37	22	34.17	0.7	3669.09	1.81	6628.82	37.89	38.14
23	184	195	220	0.89	51	58	20	38.97	0.76	4771.96	2.07	9877.95	44.18	44.4
24	201	170	112	1.52	53	41	31	40.69	0.77	5203.46	1.44	7510.32	49.94	50.42
25	194	280	258	1.09	62	49	22	40.58	0.65	5176.28	1.42	7333.07	34.05	32.18
<b>AVERAGE</b>	276.12	357.48	329.28	1.13	60.08	50.56	29.16	44.22	0.74	6293.18	1.86	12319.04	78.68	71.77

**Appendix A2: UMUCAS-37 Variety**

Sample	L (mm)	M <sub>c</sub> (g)	V <sub>c</sub> cm <sup>3</sup>	ρ <sub>s</sub> (g/cm <sup>3</sup> )	R <sub>th</sub> (mm)			GMD (mm)	Sphericity φ	S <sub>a</sub> (mm <sup>2</sup> )	P <sub>th</sub> (mm)	V <sub>p</sub> (mm <sup>3</sup> )	M <sub>Pt</sub> (g)	M <sub>Pa</sub> (g)
					a	b	c							
1	490	326	346	0.94	78	63	28	51.63	0.66	8376.32	2.92	24458.86	157.97	89.88
2	401	1666	1683	0.98	83	61	39	58.23	0.70	10657.12	2.87	30550.40	151.52	116.76
3	320	423	486	0.87	79	71	48	64.57	0.82	13104.16	2.75	35992.75	129.70	122.18
4	336	458	476	0.96	66	45	28	43.65	0.66	5987.80	3.18	19021.26	98.90	71.38
5	355	420	490	0.85	74	56	29	49.35	0.67	7653.67	2.50	19159.69	83.91	63.51
6	325	1212	1309	0.93	84	66	33	56.77	0.68	10128.60	1.83	18569.10	71.48	67.05
7	245	1140	1148	0.99	73	70	41	59.39	0.81	11086.50	2.43	26903.24	92.59	94.19
8	298	519	600	0.87	40	47	31	38.77	0.97	4724.30	1.82	8598.23	56.21	39.01
9	266	1008	1017	0.99	69	63	44	57.62	0.84	10433.25	2.56	26743.89	104.05	103.38
10	271	1395	1421	0.98	43	37	30	36.27	0.84	4135.41	3.50	14473.95	90.52	75.42
11	220	1215	1200	1.01	56	60	28	45.48	0.81	6501.14	2.33	15147.66	63.59	59.81
12	348	910	930	0.97	33	30	16	25.11	0.76	1982.26	2.32	4592.24	49.25	22.37
13	297	699	687	1.01	40	47	31	38.77	0.97	4724.30	1.95	9196.64	69.97	56.23
14	255	201	247	0.81	75	72	34	56.84	0.76	10152.50	2.00	20271.16	59.54	54.33
15	310	1070	1086	0.98	49	48	16	33.51	0.68	3529.36	2.20	7776.36	54.19	29.72
16	396	479	491	0.96	83	73	29	56.01	0.67	9859.55	2.54	25043.27	126.29	93.76
17	305	135	153	0.89	66	36	27	40.03	0.61	5036.53	2.00	10073.06	44.50	34.96
18	155	114	127	0.86	72	64	36	54.95	0.76	9488.58	2.35	22329.79	43.14	44.89
19	167	395	457	0.86	48	44	28	38.96	0.81	4770.45	2.94	14025.12	43.30	42.28
20	198	135	154	0.88	36	34	13	25.15	0.70	1988.27	2.92	5812.36	30.83	29.87
21	167	251	282	0.89	30	27	17	23.97	0.80	1805.57	2.34	4219.01	21.51	18.65
22	228	175	207	0.85	74	64	42	58.37	0.79	10709.40	1.93	20669.15	55.34	54.15
23	308	340	374	0.91	68	34	20	35.89	0.53	4048.90	2.05	8300.23	38.72	29.43
24	236	965	1004	0.96	69	60	20	43.59	0.63	5970.51	1.89	11284.27	42.27	42.30
25	230	445	532	0.83	67	63	32	51.31	0.77	8273.73	1.87	15444.30	46.31	49.99
<b>AVERAGE</b>	285.08	430.24	467.65	0.92	62.20	53.40	29.60	45.77	0.75	7005.13	2.40	16746.24	73.02	65.79

## Appendix A3: UMUCAS 38 Variety

Sample	L (mm)	M <sub>c</sub> (g)	V <sub>c</sub> (cm <sup>3</sup> )	ρ <sub>s</sub> (g/cm <sup>3</sup> )	R <sub>th</sub> (mm)			GMD (mm)	Sphericity φ	S <sub>a</sub> (mm <sup>2</sup> )	P <sub>th</sub> (mm)	V <sub>p</sub> (mm <sup>3</sup> )	M <sub>Pt</sub> (g)	M <sub>Pa</sub> (g)
					a	b	c							
1	243	388	388	1.00	51	60	33	46.57	0.91	6815.56	2.43	17720.45	81.23	82.40
2	259	480	474	1.01	41	38	34	37.56	0.92	4433.11	2.47	11526.09	70.25	64.27
3	478	256	238	1.08	74	66	42	58.98	0.80	10931.87	3.06	39573.36	238.81	197.93
4	457	615	510	1.21	73	47	24	43.51	0.60	5948.84	2.71	16716.24	134.10	123.73
5	216	2033	1960	1.04	63	61	58	60.63	0.96	11554.29	2.37	31312.13	97.30	93.60
6	598	758	770	0.98	80	54	28	49.46	0.62	7687.27	2.38	20448.14	146.99	141.02
7	314	416	246	1.69	56	48	24	40.11	0.72	5055.58	2.52	14509.53	128.34	124.09
8	250	189	151	1.25	51	42	24	37.18	0.73	4345.42	2.92	15817.32	81.56	82.06
9	339	473	443	1.07	63	46	26	42.24	0.67	5606.94	2.36	13849.13	80.88	78.76
10	263	409	346	1.18	71	62	38	55.10	0.78	9541.87	2.27	29007.28	98.11	101.49
11	444	1018	979	1.04	62	62	32	49.73	0.80	7773.80	2.52	20989.26	152.32	159.44
12	186	302	348	0.87	49	40	25	36.59	0.75	4208.64	3.27	14141.03	47.08	47.06
13	353	392	367	1.07	51	46	25	38.85	0.76	4744.49	2.43	13426.91	89.33	86.69
14	200	404	375	1.08	48	43	23	36.21	0.75	4120.68	1.76	8076.54	34.10	40.46
15	378	977	805	1.21	52	46	32	42.46	0.82	5666.11	2.07	13655.33	105.43	109.27
16	195	934	868	1.08	68	58	31	49.63	0.73	7742.42	2.58	25162.87	65.07	70.90
17	205	686	625	1.10	58	57	41	51.37	0.89	8293.46	2.02	17499.19	65.79	79.31
18	360	1226	1112	1.10	50	38	22	34.71	0.69	3785.55	1.99	7381.82	63.07	57.84
19	267	333	374	0.89	86	75	43	65.21	0.76	13366.87	1.85	28337.77	71.27	71.33
20	321	786	708	1.11	83	74	46	65.62	0.79	13532.86	2.37	36538.71	141.80	138.48
21	210	615	510	1.21	46	43	25	36.70	0.80	4234.37	2.63	11940.92	63.55	66.96
22	276	807	778	1.04	78	62	37	56.35	0.72	9980.13	2.11	22654.91	80.79	77.06
23	537	974	911	1.07	67	57	24	45.09	0.67	6389.28	3.23	23832.00	193.69	188.62
24	243	337	312	1.08	53	42	28	39.65	0.75	4940.83	2.02	10276.92	51.11	51.62
25	410	541	549	0.99	58	43	21	37.41	0.65	4399.68	2.39	11747.16	79.50	78.83
<b>AVERAGE</b>	<b>320.08</b>	<b>497.96</b>	<b>452.69</b>	<b>1.10</b>	<b>61.28</b>	<b>52.40</b>	<b>31.44</b>	<b>46.28</b>	<b>0.76</b>	<b>7004.00</b>	<b>2.43</b>	<b>19045.64</b>	<b>98.46</b>	<b>96.37</b>

## Appendix A4: TMS 30572 Variety

Sample	L (mm)	M <sub>c</sub> (g)	V <sub>c</sub> (cm <sup>3</sup> )	ρ <sub>s</sub> (g/cm <sup>3</sup> )	R <sub>th</sub> (mm)			GMD (mm)	Sphericity φ	S <sub>a</sub> (mm <sup>2</sup> )	P <sub>th</sub> (mm)	V <sub>p</sub> (mm <sup>3</sup> )	M <sub>Pt</sub> (g)	M <sub>Pa</sub> (g)
					a	b	c							
1	340	250	186	1.34	85	81	55	72.35	0.85	16450.87	1.87	30817.96	168.70	157.40
2	314	285	245	1.16	65	63	51	59.33	0.91	11063.53	2.12	23491.56	132.75	103.84
3	290	375	247	1.52	47	44	19	34.00	0.72	3632.57	2.43	8815.03	89.06	50.86
4	461	295	273	1.08	79	67	60	68.23	0.86	14630.07	2.28	33356.57	211.68	136.97
5	220	195	140	1.39	47	44	31	40.02	0.85	5034.46	2.17	10924.77	72.37	57.82
6	460	225	196	1.15	66	66	53	61.35	0.93	11828.24	2.36	27954.08	224.82	121.94
7	355	280	258	1.09	67	67	47	59.53	0.89	11138.91	2.02	22537.73	131.34	92.95
8	263	610	565	1.08	62	54	43	52.41	0.85	8633.37	2.76	23856.88	110.48	97.88
9	298	305	273	1.12	51	48	24	38.88	0.76	4749.99	2.26	10719.15	73.80	55.51
10	286	645	575	1.12	53	53	43	49.43	0.93	7679.94	2.76	21222.24	129.07	90.46
11	265	410	396	1.04	66	63	43	56.34	0.85	9975.00	2.47	24671.51	104.37	97.07
12	225	921	1035	0.89	57	45	44	48.33	0.85	7340.14	2.22	16270.65	57.55	55.02
13	198	820	806	1.02	63	64	43	55.76	0.89	9772.46	2.05	20033.53	65.09	67.45
14	258	575	500	1.15	63	68	48	59.02	0.94	10949.77	2.64	28943.88	137.79	126.48
15	322	545	534	1.02	56	58	44	52.28	0.93	8591.26	2.23	19187.15	113.42	74.41
16	354	480	356	1.35	73	69	47	61.86	0.85	12027.93	2.26	27143.03	180.73	139.07
17	365	240	190	1.26	83	75	37	61.30	0.74	11809.69	1.73	20391.40	120.11	97.88
18	240	545	405	1.35	65	64	41	55.46	0.85	9666.35	2.18	21040.42	106.82	107.59
19	263	435	382	1.14	62	54	43	52.41	0.85	8633.37	2.12	18331.52	89.54	79.32
20	235	340	270	1.26	67	63	32	51.31	0.77	8274.11	3.07	25401.52	118.07	121.55
21	275	580	491	1.18	59	54	28	44.68	0.76	6275.00	2.36	14829.91	85.88	66.57
22	366	1790	1685	1.06	54	51	28	42.56	0.79	5694.11	2.37	13476.06	101.06	54.40
23	363	425	300	1.42	53	52	46	50.24	0.95	7931.75	1.97	15651.99	152.16	84.26
24	349	410	272	1.51	54	51	20	38.05	0.70	4549.95	2.36	10753.06	114.71	61.59
25	230	500	514	0.97	58	57	38	50.08	0.86	7883.80	2.31	18185.29	71.43	67.22
<b>AVERAGE</b>	<b>303.80</b>	<b>499.24</b>	<b>419.76</b>	<b>1.19</b>	<b>62.20</b>	<b>59.00</b>	<b>40.32</b>	<b>52.61</b>	<b>0.85</b>	<b>8968.67</b>	<b>2.30</b>	<b>20320.27</b>	<b>118.51</b>	<b>98.6208</b>

## Appendix A5: TME 419 Variety

Sample	L (mm)	M <sub>c</sub> (g)	V <sub>c</sub> (cm <sup>3</sup> )	ρ <sub>s</sub> (g/cm <sup>3</sup> )	R <sub>th</sub> (mm)			GMD (mm)	Sphericity φ	S <sub>a</sub> (mm <sup>2</sup> )	P <sub>th</sub> (mm)	V <sub>p</sub> (mm <sup>3</sup> )	M <sub>Pt</sub> (g)	M <sub>Pa</sub> (g)
					a	b	c							
1	329	830	721	1.15	69	63	30	50.71	0.73	8082.61	2.66	21472.80	125.50	106.79
2	278	545	507	1.07	67	50	25	43.75	0.65	6016.37	2.85	17146.64	82.74	79.63
3	390	1000	916	1.09	80	70	27	53.27	0.67	8920.29	3.33	29674.83	174.90	139.95
4	371	715	662	1.08	68	60	32	50.73	0.75	8088.81	3.74	30225.18	187.24	184.03
5	282	835	726	1.15	74	67	42	59.27	0.80	11042.01	3.37	37174.78	167.68	146.71
6	409	630	567	1.11	54	46	24	39.06	0.72	4796.45	3.28	15748.33	140.22	125.59
7	240	565	225	2.51	63	54	33	48.24	0.77	7314.36	2.83	20724.03	205.47	204.81
8	317	620	560	1.11	58	54	32	46.45	0.80	6781.50	2.57	17428.45	108.97	93.36
9	260	445	413	1.08	58	51	22	40.22	0.69	5085.01	2.86	14543.12	76.26	67.69
10	228	630	547	1.15	67	70	50	61.67	0.92	11951.97	3.31	39521.19	156.57	156.64
11	276	470	428	1.10	65	48	22	40.94	0.63	5269.01	2.90	15280.14	78.30	72.49
12	255	380	298	1.28	52	49	24	39.40	0.76	4878.48	2.42	11822.19	78.18	65.13
13	356	645	600	1.08	58	47	30	43.41	0.75	5921.65	3.23	19107.18	130.70	113.73
14	251	495	388	1.28	61	55	32	47.53	0.78	7099.69	2.87	20399.78	111.15	112.43
15	290	665	598	1.11	69	64	35	53.67	0.78	9051.96	3.18	28785.22	140.38	138.28
16	162	340	305	1.11	61	55	25	43.77	0.72	6022.35	2.44	14714.61	46.77	45.86
17	325	485	378	1.28	54	47	23	38.79	0.72	4729.60	2.73	12911.80	106.23	79.57
18	236	475	427	1.11	64	63	26	47.15	0.74	6987.80	2.58	18051.81	80.09	81.75
19	221	455	374	1.22	53	63	31	46.95	0.89	6928.88	2.67	18523.21	98.06	97.35
20	267	535	459	1.17	70	51	32	48.52	0.69	7399.85	2.94	21780.24	101.77	101.67
21	298	740	685	1.08	76	63	22	47.23	0.62	7010.18	3.62	25400.20	122.26	118.54
22	295	755	700	1.08	64	60	35	51.22	0.80	8246.64	2.96	24437.55	125.70	113.87
23	193	320	278	1.15	55	53	40	48.85	0.89	7501.42	2.58	19378.67	79.04	76.36
24	295	290	268	1.08	50	35	20	32.71	0.65	3362.97	2.12	7118.29	48.62	43.28
25	217	275	214	1.29	50	44	31	40.86	0.82	5246.47	2.46	12888.83	73.30	71.55
<b>AVERAGE</b>	<b>281.64</b>	<b>565.60</b>	<b>471.76</b>	<b>1.20</b>	<b>62.40</b>	<b>55.28</b>	<b>29.80</b>	<b>46.58</b>	<b>0.75</b>	<b>6949.45</b>	<b>2.90</b>	<b>20570.36</b>	<b>113.84</b>	<b>105.88</b>

APPENDIX B

Equation of Model Format

REF: Computer Simulation for Predicting Efficiency of Cassava Attrition Peeling Machine

$F_t$  = Tangential force

$F_f$  = Frictional force

$F_N$  = Normal force

$Mg$  = weight of the particle

$T_d$  = Torque on the drum

$R_d$  = Radius of the drum

$$\eta_p = \frac{p_w \varphi_c D_g \left( \frac{1,2k\rho_p \pi n_d R_d \left[ \left( \frac{30P_d}{\pi N_d R_d} \right) - (m_c + nm_b) g \sin \theta \right] \pi N_s r_d \left| \pi R_d (R_d + L_d) - \left\{ 2\pi n_b a^2 + \pi n_b a \left[ \frac{b^2}{\sqrt{b^2 - a^2}} \cos^{-1} \left( \frac{a}{b} \right) + \frac{c^2}{\sqrt{c^2 - a^2}} \cos^{-1} \left( \frac{a}{c} \right) \right\} \right| \right)}{\mu(30P_d)} \right)}{P_{th}(M_r + p_w \left( \frac{1,2k\rho_p \pi n_d R_d \left[ \left( \frac{30P_d}{\pi N_d R_d} \right) - (m_c + nm_b) g \sin \theta \right] \pi N_s r_d \left| \pi R_d (R_d + L_d) - \left\{ 2\pi n_b a^2 + \pi n_b a \left[ \frac{b^2}{\sqrt{b^2 - a^2}} \cos^{-1} \left( \frac{a}{b} \right) + \frac{c^2}{\sqrt{c^2 - a^2}} \cos^{-1} \left( \frac{a}{c} \right) \right\} \right| \right)}{\mu(30P_d)} \right))}$$

1.  $1,2k\rho_p \pi n_d R_d$  var (233.5) - meaning (Deposit constant)
2.  $\frac{30P_d}{\pi N_d R_d}$  Constant (23.093)
3.  $(m_c + nm_b) g \sin \theta$  Var ( M , Nm, gism )  $\geq 65 \leq 90$
4.  $\pi N_s r_d$  Var (Ns, rd , )
5.  $\pi R_d (R_d + L_d)$  Var ( Rd, Ld )
6.  $2\pi n_b a^2 + \pi n_b a$  Var (nb, a ) nb - number of balls
7.  $\frac{b^2}{\sqrt{b^2 - a^2}} \cos^{-1} \left( \frac{a}{b} \right) + \frac{c^2}{\sqrt{c^2 - a^2}} \cos^{-1} \left( \frac{a}{c} \right)$  Var ( b, a, c  $\cos^{-1} = 0.003647$ )
8.  $P_{th}(M_r + p_w)$  Var ( Pth, Mr, Pw)
9.  $1,2k\rho_p \pi n_d R_d$  Var ( kpp nd, Pie, Rd )
10.  $\left( \frac{30P_d}{\pi N_d R_d} \right)$  Var ( pd , Pie , Nd, Rd )
11.  $\left[ \left( \frac{30P_d}{\pi N_d R_d} \right) - (m_c + nm_b) g \sin \theta \right] \pi N_s r_d$  Var ( Pd, Pie, Nd, Rd, Mc, Nmb, gSin, Ns, rd)
12.  $\pi R_d (R_d + L_d)$
13.  $2\pi n_b a^2 + \pi n_b a$
14.  $\frac{b^2}{\sqrt{b^2 - a^2}} \cos^{-1} \left( \frac{a}{b} \right)$
15.  $\frac{c^2}{\sqrt{c^2 - a^2}} \cos^{-1} \left( \frac{a}{c} \right)$
16.  $\mu(30P_d)$

**APPENDIX C**

```

%      MATLAB PROGRAM FOR IMPROVED MACHINE
%      PEELING EFFICIENCY OF CASSAVA ATTRITION PEELING MACHINE (CAPM)
Pw = input('peeling weight proportion (%) ');
a1 = input('cassava major diameter (m) ');
Sp = input('cassava sphericity(%) ');
Dg = a1*Sp;
k = 0.08;
Dp = 1100;
Nd = input('drum speed (r/min) ');
nd = input('number of rev. of drum ');
Rd = 0.38;
g = 9.81;
v = (pi*Rd*Nd)/30;
ad = v/120;
Md = 7;
Mb = 0.05;
nb = input('number of peeling balls ');
Mc = input('mass of cassava (kg) ');
Ft = (Md+Mc+nb*Mb)*ad;
Td = Ft*Rd;
tita = input('Angle of repose(deg.)');
Ff = Ft - (Mc+nb*Mb)*g*sin(tita);
U = input('coefficient of friction ');
Pd = (pi*Nd*Td)/30;
Ld = 0.635;
Sad = pi*Rd*(Rd+Ld);
a = 0.002;
b = 0.0022;
c = 0.0032;
Sab = 2*pi*nb*a^2+pi*nb*a*((b^2*cos(a/b)/sqrt(b^2-a^2))+(c^2*cos(a/c)/sqrt(c^2-a^2)));
Stc = Sad - Sab;
Pth = input('Peel thickness (m)');
Mr = input('mass of peel removed by hand (kg)');
T = input('Ambient temperature (deg.)');
h = input('Humidity (%) ');
x = 0.026-0.0045*h+0.01215*T;
y = 0.013362 + 0.194*h-0.00017*h^2+0.009468*T;
t = 60;
MR = exp(-x*t^y);
A = 727.44*h + 599.9*h^2 + 475.64*h^3;
B = -0.0143 - 0.000771*h + 0.132*h^2 - 0.157*h^3 - 0.0731*h^4;
C = T + 81.64;

```

```

M1 = input('initial moisture content(%');
Me = 0.01*A*exp(B*C);
Mt = (exp(-x*t^y)*(M1 - Me) + Me)/100;
Efficiency = (Pw*Mt*Dg*(1.2*pi^2*k*Dp*Nd*Rd^2*Stc*((30*Pd/pi*Nd*Rd)-
(Mc+nb*Mb)*g*sin(tita)))/(Pth*(30*U*Pd*Rd+Pw*(1.2*pi^2*k*Dp*Nd*Rd^2*Stc*((30*Pd/pi*Nd*Rd)-
(Mc+nb*Mb)*g*sin(tita))))

```